# Electrochemical Studies of Complexes with Oxo- or Hydroxo-Bridged $\{Mo_2(\mu\text{-}SMe)_3\}^+$ Centers: Cleavage of the Oxygen Bridge and Generation of Substrate-Binding Sites

**Marc Le Hénanf,[a] Christine Le Roy,[a] Kenneth W. Muir,[b] François Y. Pétillon,[a] Philippe Schollhammer,[a] and Jean Talarmin*[a]**

**Keywords:** Dinuclear complexes / Molybdenum / Electrochemical reduction / Oxo, hydroxo bridges / Protonations / Aqua ligands

The reduction of $[Mo_2(Cp)_2(\mu\text{-}SMe)_3(\mu\text{-}O)]^+$ (**1**$^+$) has been investigated by cyclic voltammetry and controlled-potential electrolysis in THF- and MeCN/$NBu_4PF_6$ without added acid or in the presence of various acids HX (HX: HTsO, $CF_3CO_2H$, $HBF_4$). Reduction in the presence of acid follows an $EC_{rev}E$ mechanism in which the intermediate chemical step is an acid-base equilibrium between **1** and $[Mo_2(Cp)_2(\mu\text{-}SMe)_3(\mu\text{-}OH)]^+$ (**2**$^+$). This electrochemical process is followed by protonation of the neutral μ-hydroxo complex **2** to afford different products which depend both on the solvent (THF or MeCN) and on the nature of the acid. Controlled-potential electrolysis of **1**$^+$ in the presence of HX (2 equiv.) leads to the generation of binding sites and finally gives products identical to those obtained from protonation of **2** by HX. The complex $[Mo_2(Cp)_2(\mu\text{-}SMe)_3(\mu\text{-}\eta^1,\eta^1\text{-}OCOCF_3)]$ (**3**) which can be obtained either by protonation of **2** by $CF_3CO_2H$ or by reduction of **1**$^+$ in the presence of $CF_3CO_2H$, has been characterized crystallographically. In the presence of $HBF_4$ protonation of **1**$^+$ gives **2**$^{2+}$. The reactivity of **2**$^+$ and of the complexes $[Mo_2(Cp)_2(\mu\text{-}SMe)_3(H_2O)(TsO)]$ (**4**) and $[Mo_2(cp)_2(\mu\text{-}SMe)_3(H_2O)L]^+$ (L = $H_2O$ or THF) (**6**$^+$), all of which contain a terminal aqua ligand, has also been investigated.


## Introduction

We have previously reported various aspects of the chemistry and electrochemistry of dinuclear complexes in which the metal centers are held together by thiolate bridges.[1] We have shown that the dinuclear $\{[Mo_2(Cp)_2(\mu\text{-}SMe)_3]^+\}$ entity can sustain progressive reduction of nitrogenous substrates thus modeling, in vitro, key steps of the nitrogen fixation process.[2−7] The same dinuclear center also permits the conversion of alkynes to carbyne and alkyl groups[8] and the partial reduction of C≡N bonds.[9] These transformations are facilitated by the ability of the $\{[Mo_2(Cp)_2(\mu\text{-}SMe)_3]^+\}$ core to adapt to the different modes of coordination required by different substrates. Recently, we turned our attention to oxygen-containing complexes such as $[Mo_2(Cp)_2(\mu\text{-}SMe)_3(\mu\text{-}O)]^+$ (**1**$^+$) and $[Mo_2(Cp)_2(\mu\text{-}SMe)_3(\mu\text{-}OH)]$ (**2**) (respectively isoelectronic with the imido and amido complexes we studied previously[5,6]) to see whether they had potential as precursors to species with sites able to bind and reduce nitrate and nitrite.[10]

Much of the published work on dinuclear complexes containing oxo- and/or hydroxo bridges has been prompted by the implication of such centers in various biological processes.[11] Electrochemical studies have been published for iron, ruthenium and manganese compounds.[12−14] In the case of molybdenum it has been reported that chemical reduction of a dinuclear complex with terminal and bridging oxo groups in acidic aqueous media affords complexes with hydroxo or aqua ligands,[15] and electrochemical studies of complexes with the $Mo_2O_2(\mu\text{-}O)_2^{2+}$ core in various aqueous buffers have shown that the terminal oxo groups are reduced to aqua ligands.[16]

In this paper, we report detailed electrochemical studies of the reactivity at the oxygen bridges in **1**$^+$ and **2**. We show that by protonation of **2** or reduction of **1**$^+$ in acidic solution it is possible to generate coordination sites suitable for occupation by oxygen-donor ligands such as the trifluoroacetate anion. Related to this, the crystal and molecular structures of $[Mo_2(Cp)_2(\mu\text{-}SMe)_3(\mu\text{-}\eta^1,\eta^1\text{-}OCOCF_3)]$ are described. The reactivity at the μ-oxo and μ-hydroxo ligands is shown to be strongly affected by the (formal) oxidation state of the metal centers in the $\{Mo(\mu\text{-}SMe)_3\}$ core. We believe that these results, obtained for dimolybdenum species, may also provide a more general insight into the reactivity of oxo and hydroxo groups when they act in a bridging role at a dinuclear metal center.

[a] UMR CNRS 6521 Chimie, Electrochimie Moléculaires et Chimie Analytique, Université de Bretagne Occidentale
6 Av. V. Le Gorgeu, 29285 Brest Cedex, France
E-mail: jean.talarmin@univ-brest.fr
[b] Department of Chemistry, University of Glasgow
Glasgow G12 8QQ, UK

## Results and Discussion

In order to examine the reactivity of the bridging oxo ligand the electrochemical reduction of $\mathbf{1}^+$ was investigated in the absence and presence of acid (tetrafluoroboric: $HBF_4/H_2O$ or $HBF_4/Et_2O$; trifluoroacetic: $CF_3CO_2H$; *p*-toluenesulfonic: HTsO) using THF- or $MeCN/NBu_4PF_6$ as an electrolyte. Because the presence of acid is likely to lead to protonation at the oxygen bridge, we also investigated the reactivity of $[Mo_2(Cp)_2(\mu\text{-}SMe)_3(\mu\text{-}OH)]$ (**2**) with acids and its oxidative electrochemistry. For the sake of clarity, this topic is presented first.

### 1. Protonation and Oxidation of $[Mo_2(Cp)_2(\mu\text{-}SMe)_3(\mu\text{-}OH)]$ (2)

The μ-hydroxo complex **2** was prepared by our standard method[10] which involves treatment of $[Mo_2(Cp)_2(\mu\text{-}SMe)_3(\mu\text{-}Cl)]$[17] with an excess of KOH. This reaction produced samples of **2** contaminated with small amounts of other compounds. Repeated attempts to purify these samples failed because **2** has limited stability in solution and decomposes during column chromatography. The reactivity studies were therefore carried out with samples of **2** containing small quantities of impurities (see Figure 1,a).

#### *Protonation of $[Mo_2(Cp)_2(\mu\text{-}SMe)_3(\mu\text{-}OH)]$, 2: Cleavage of the OH Bridge*

The action of acid on **2** depends both on the solvent and on the nature of the acid. Addition of 1 equivalent of $HBF_4$ to a MeCN solution of **2** quantitatively[18] produced the known[4] bis(acetonitrile) complex $\mathbf{5}^+$, identified by its characteristic redox potentials (Scheme 1). Treatment of **2** with 1 equivalent of $CF_3CO_2H$ in THF resulted in the quantitative[18] formation of $[Mo_2(Cp)_2(\mu\text{-}SMe)_3(\mu\text{-}\eta^1,\eta^1\text{-}OCOCF_3)]$ (**3**) (Scheme 1), which has been fully characterized (see Crystallographic and Experim. Sections). In both cases it is likely that initial protonation at the bridging hydroxide and binding of the conjugate base, or a solvent molecule, is followed by elimination of $H_2O$ from the undetected aqua intermediate, $[Mo_2(Cp)_2(\mu\text{-}SMe)_3(H_2O)(L/X)]^{n+}$ [X = $CF_3CO_2$, $n$ = 0; L = MeCN, $n$ = 1], to give the observed products. It should be noted that the ammine analogue of the intermediate can be obtained by protonation of $[Mo_2(Cp)_2(\mu\text{-}SMe)_3(\mu\text{-}NH_2)]$ by trifluoroacetic acid in THF but is also detectable by cyclic voltammetry as an intermediate on the path to $\mathbf{5}^+$ {obtained by protonation of $[Mo_2(Cp)_2(\mu\text{-}SMe)_3(\mu\text{-}NH_2)]$ by $HBF_4$ in MeCN}.[5] The different lifetimes of the aqua- and ammine-containing species suggest that $H_2O$ is more labile than $NH_3$ at the $\{Mo_2(Cp)_2(\mu\text{-}SMe)_3\}$ site.

Complex **2** also reacted with HTsO (Scheme 1). The reaction product **4** was formed quantitatively[18] but could not be isolated or characterized. Complex **4** was formulated as $[Mo_2(Cp)_2(\mu\text{-}SMe)_3(H_2O)(TsO)]$ by analogy with $[Mo_2(Cp)_2(\mu\text{-}SMe)_3(NH_3)(TsO)]$ which is formed through protonation of $[Mo_2(Cp)_2(\mu\text{-}SMe)_3(\mu\text{-}NH_2)]$ by HTsO in THF.[5] Since there was a possibility that the $TsO^-$ anion could occupy a bridging position (due to the lability of the aqua ligand compared with $NH_3$), we investigated the reactivity and electrochemistry of **4** in order to obtain more information about the nature of this complex.

Treatment of **4** with different substrates (MeCN, *t*BuNC, $Cl^-$, $CF_3CO_2^-$), respectively, produced $[Mo_2(Cp)_2(\mu\text{-}SMe)_3(L)_2]^+$ (L = MeCN or *t*BuNC), $[Mo_2(Cp)_2(\mu\text{-}SMe)_3(\mu\text{-}Cl)]$ or $[Mo_2(Cp)_2(\mu\text{-}SMe)_3(\mu\text{-}\eta^1,\eta^1\text{-}OCOCF_3)]$

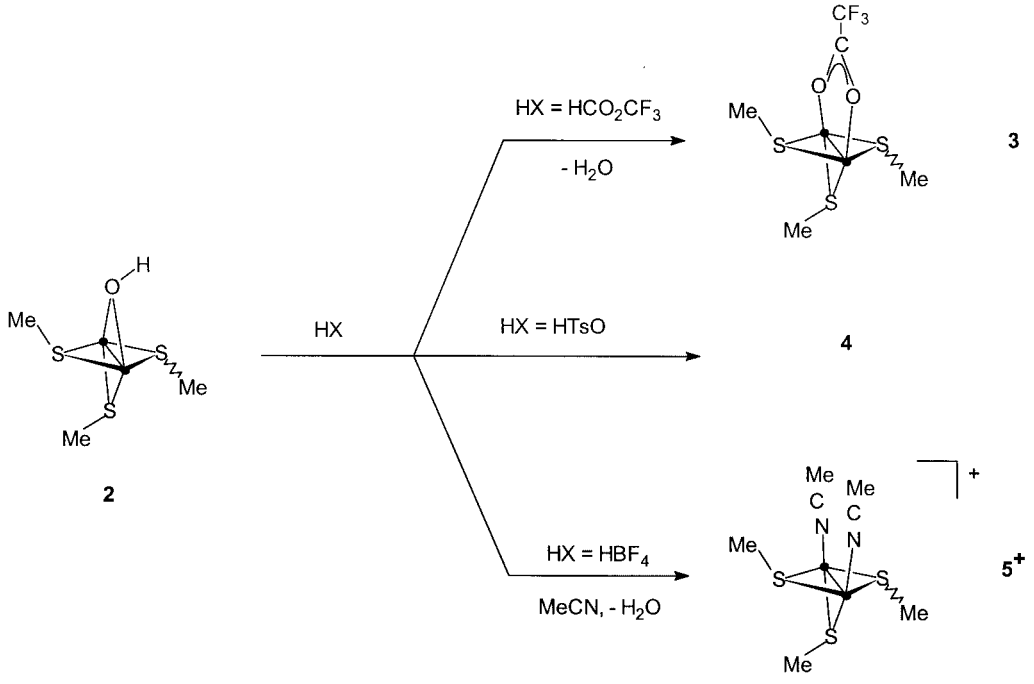


Scheme 1. • = Mo(Cp)

  

Table 1 Redox potentials of the different complexes

| Compound | Solvent | $E_{1/2}^{red1}$ [a] [V/Fc] | $E_p^{red2}$ [V/Fc] | $E_{1/2}^{ox1}$ [V/Fc] | $E_{1/2}^{ox2}$ [V/Fc] |
|---|---|---|---|---|---|
| **1**$^+$ | thf | −0.89 | −1.9 (irr) | 0.94 (irr) | − |
| | $CH_3CN$ | −0.88 | −1.7 (irr) | 0.92 (irr) | − |
| | $CH_2Cl_2$ | −0.86 | −1.9 (irr) | 1.1 (irr) | |
| **2** | thf | −3.1 (irr) | − | −0.63 (120)[b] | −0.34 (330)[b] |
| | $CH_2Cl_2$ | | | −0.58 (80)[b] | −0.15 (150)[b] |
| **3** | thf | −2.87 (irr) | | −0.35 | 0.35 |
| **4** | thf | −2.48 (irr) | | −0.51 | 0.14 |
| **6**$^+$ | thf | −2.5 (irr) | | −0.46 | 0.20 |

[a] Potentials were determined by cyclic voltammetry at a vitreous carbon electrode and a scan rate of 0.2 V·s$^{-1}$; irr: irreversible. [b] $\Delta Ep$ in mV (average) measured at $v$ = 0.2 V·s$^{-1}$.

(**3**). These products were characterized by their redox potentials (refs.[4,19] and Table 1) and, for the latter two complexes, by the NMR spectra of the solids isolated after completion of the reaction. This demonstrates that **4** retains the $\{Mo_2(Cp)_2(\mu\text{-}SMe)_3\}$ core.

The electrochemical study of **4** provided indirect evidence for the presence of an aqua ligand in the complex. Firstly, the electrochemical reduction of **4** ($E_{el}$ = −2.6 V, Pt cathode, 1 F·mol$^{-1}$ **4**) produced the hydroxo complex **2** (Scheme 2). This can be shown by comparing the CV[20] of the catholyte (Figure 2, b) with that of **2** in the presence of $TsO^-$ (Figure 1, b). The shapes of the CV curves in Figure 1(b) and Figure 2(b) arose from the reaction of complex **2**$^+$ generated at the electrode with $TsO^-$. This will be detailed below. The fact that **2** is generated by a one-electron reduction of **4** is consistent with the occurrence of an aqua ligand in the latter, but cannot be reconciled with **4** being $[Mo_2(Cp)_2(\mu\text{-}SMe)_3(\mu\text{-}OTs)]$. Secondly, the first oxidation of **4** ($E_{1/2}^{ox1}$ = −0.51 V, Table 1) shown in Figure 3(A) occurs according to an EC process[20,21] (the peak current ratio $(i_p^c/i_p^a)^{ox1}$ increases with increasing scan rates, and the product peak decreases accordingly). The product peak observed on the reverse scan can be suppressed in the presence of excess acid (Figure 3, B). This indicates that the electrochemical oxidation of **4** follows an $EC_{rev}$ mechanism,[21] as shown in Scheme 2, the chemical step being a *reversible* proton loss from **4**$^+$. Since treatment of **2**$^+$ with HTsO afforded **4**$^+$ (see below), these results are entirely consistent with **4** being $[Mo_2(Cp)_2(\mu\text{-}SMe)_3(H_2O)(TsO)]$.

Treatment of **2** with 1 equivalent of $HBF_4/H_2O$ in THF resulted in partial oxidation of the starting material. When the reaction was monitored by voltammetry at a rotating disc electrode, a reduction current was detected thereby showing that some **2**$^+$ had been produced. However, **2** was not entirely converted into **2**$^+$. Cyclic voltammetry of a solution of **2** in the presence of increasing amounts of $HBF_4/H_2O$ (1−5 equiv.) showed that new redox systems slowly increased at the expense of those due to the **2**$^{2+}$/**2**$^+$ and **2**$^+$/**2** couples (see below, oxidation of **2**). The new product **6**$^+$ ($E_{1/2}^{ox1}$ = −0.46 V and $E_{1/2}^{ox2}$ = 0.20 V, Table 1),

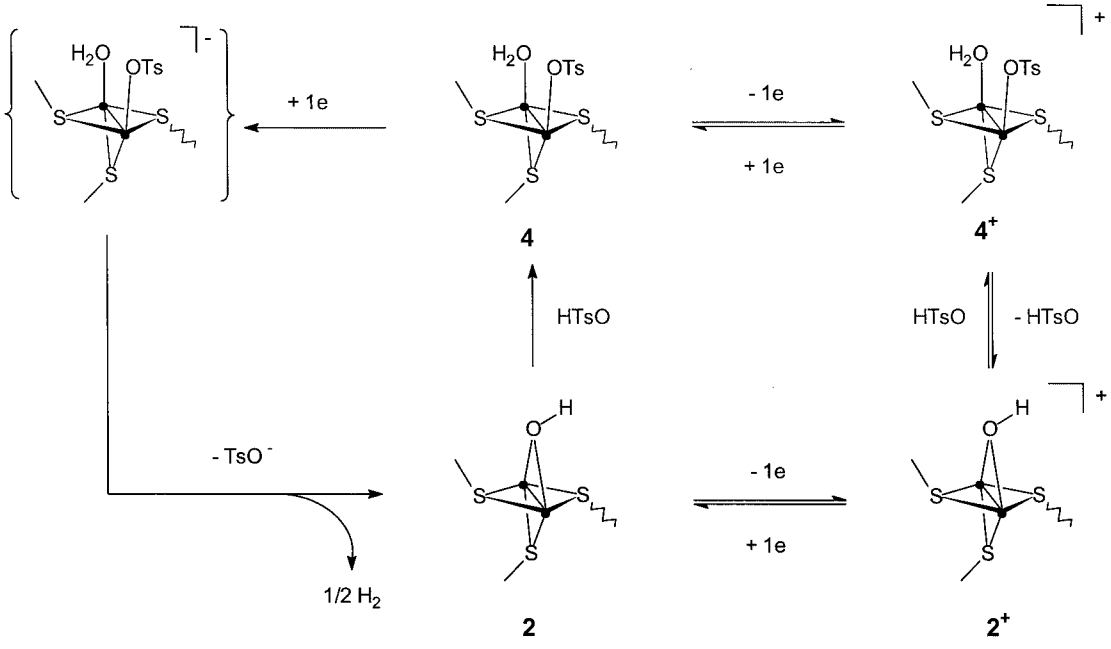


Scheme 2. • = Mo(Cp); methyl groups on the bridging S atoms are omitted

  

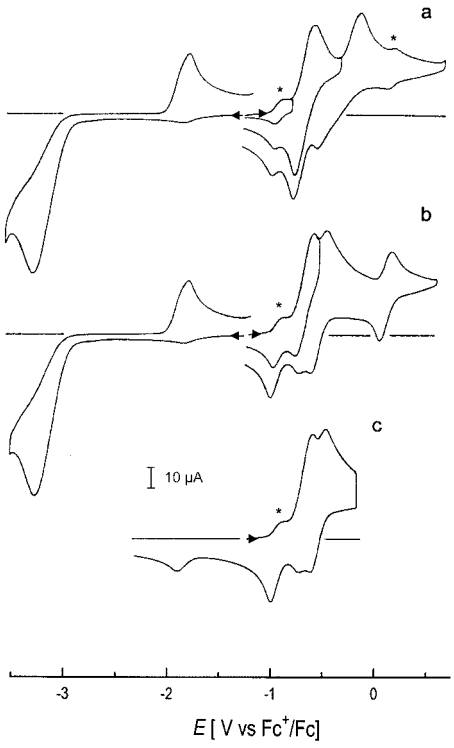


Figure 1. Cyclic voltammetry of $[Mo_2(Cp)_2(\mu\text{-}SMe)_3(\mu\text{-}OH)]$ **2** (ca. 1.2 mM) a) in the absence, and b) and c) in the presence of an excess $NBu_4TsO$. In scan c) the potential was held 10s at 0 V before scan reversal; under these conditions, the second (irreversible) reduction of $\mathbf{1}^+$ was observed on the reverse scan. The peaks marked with an asterisk are due to an impurity ($THF/NBu_4PF_6$; vitreous carbon electrode; scan rate $v = 0.2\ V{\cdot}s^{-1}$).

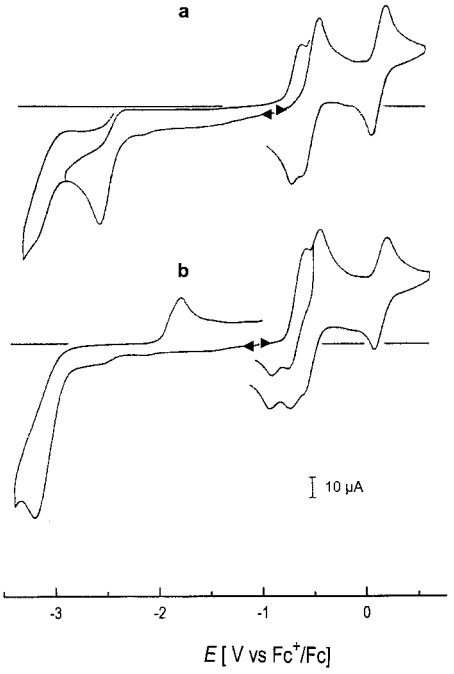


Figure 2. Cyclic voltammetry of $[Mo_2(Cp)_2(\mu\text{-}SMe)_3(H_2O)(TsO)]$ **4** (ca. 1.2 mM) a) before, and b) after electrolysis at −2.6 V ($n$ = 1 $F{\cdot}mol^{-1}$ **4**) ($THF/NBu_4PF_6$; vitreous carbon electrode; scan rate $v = 0.2\ V{\cdot}s^{-1}$).

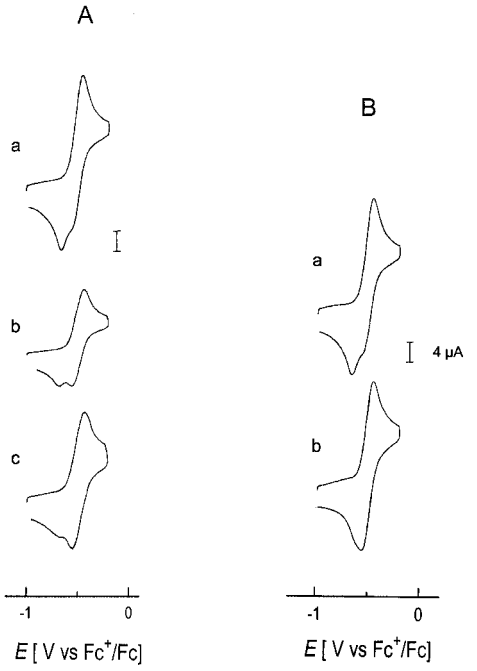


Figure 3. **A:** Cyclic voltammetry of $[Mo_2(Cp)_2(\mu\text{-}SMe)_3(H_2O)(TsO)]$ (**4**) (ca. 1.2 mM) at different scan rates a) 0.2 $V{\cdot}s^{-1}$, b) 0.5 $V{\cdot}s^{-1}$, c) 1 $V{\cdot}s^{-1}$; the current scale is 4 µA for a) and 10 µA for b) and c). **B:** Cyclic voltammetry of $[Mo_2(Cp)_2(\mu\text{-}SMe)_3(H_2O)(TsO)]$ (**4**) (ca. 1.2 mM) at $v = 0.2\ V{\cdot}s^{-1}$, a) in the absence and b) in the presence of an excess of HTsO ($THF/NBu_4PF_6$; vitreous carbon electrode)

obtained as a mixture of $\mathbf{6}^+$ and $\mathbf{6}^{2+}$, formed faster when $HBF_4/Et_2O$ replaced $HBF_4/H_2O$ in the reaction with **2**. Complex $\mathbf{6}^+$ decomposed on workup and could not be isolated or characterized by analytical methods. However, its reactivity with different substrates demonstrated the presence of labile ligand(s) bound to the metal centers of the conserved $\{[Mo_2(Cp)_2(\mu\text{-}SMe)_3]^+\}$ core and showed a striking similarity to that of complex **4**. Addition of chloride, trifluoroacetate or acetonitrile causes the quantitative conversion[18] of $\mathbf{6}^+$ to $[Mo_2(Cp)_2(\mu\text{-}SMe)_3(\mu\text{-}Cl)]$, **3** or $\mathbf{5}^+$, respectively. Furthermore, treatment of $\mathbf{6}^+$ with *t*BuNC produces the bis(isocyanide)[19] analogue of $\mathbf{5}^+$. Since the electrochemical behaviour of $\mathbf{6}^+$, and in particular its first oxidation step, is very similar to that of **4** ($EC_{rev}$ process, see Scheme 2), and since treatment of $\mathbf{2}^+$ with $HBF_4/H_2O$ afforded $\mathbf{6}^{2+}$ (see below), we have assigned $\mathbf{6}^+$ as $[Mo_2(Cp)_2(\mu\text{-}SMe)_3(H_2O)(L)]^+$, where L could be a molecule of water or THF.

Protonation at the µ-OH ligand of **2** by HX could initially produce an intermediate with an aqua bridge (Scheme 3, step A). Subsequent coordination of the conjugate base $X^-$ (or that of a substrate such as MeCN or *t*BuNC) would shift the $H_2O$ ligand from a bridging to a terminal position (Scheme 3, step B). Protonation of a hydroxo bridge in tris-bridged cobalt complexes was similarly assumed to involve a µ-aqua intermediate on the path to the final product which contained terminally coordinated $H_2O$ molecules.[22,23] Although we are not aware of stable

  

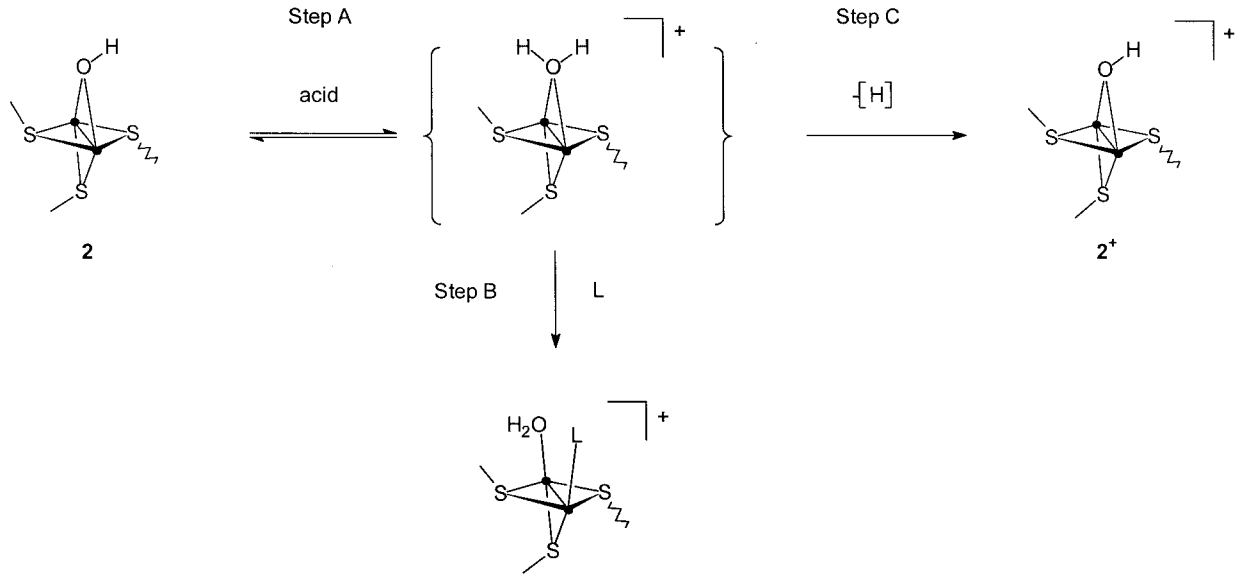


Scheme 3. • = Mo(Cp); L = MeCN, *t*BuNC, THF or $H_2O$ (see text); methyl groups on the bridging S atoms are omitted

Mo(μ-$H_2O$)Mo compounds, ruthenium,[24−26] cobalt,[27] and nickel[27] complexes containing bridging water molecule(s) have been characterized crystallographically. In these complexes, the aqua bridge appears to be stabilized via hydrogen bonds to the oxygen atom of terminally coordinated carboxylate ligands.[24−27]

Alternatively, protonation at the oxygen of **2** with concerted binding of $X^-$ would afford directly $[Mo_2(Cp)_2(\mu\text{-}SMe)_3(H_2O)(X)]$ (X = TsO or $CF_3CO_2$). This species was not detected when X = $CF_3CO_2$ but it was the final product **4** when X = TsO. In the absence of $X^-$ or ligand L (protonation by $HBF_4/H_2O$ in THF), treatment of **2** with protons led to two different types of reaction (oxidation and protonation). This suggests that two mechanisms are involved.

Although no kinetic measurements were performed, it appears that the rate of formation of $[Mo_2(Cp)_2(\mu\text{-}SMe)_3(H_2O)(L)]^+$ (Scheme 3), which is either a likely intermediate (L = MeCN, *t*BuNC) or the final product (L = $H_2O$ or THF) of the protonation of **2** under different conditions, depends on the nature of both the acid (Scheme 3, step A) and of the nucleophile (Scheme 3, step B). The nature of the acid (HX) affects the concentration of the μ-aqua intermediate by perturbing the equilibrium constant [$K_{eq} = K_a^{HX}/K_a^{(\mu\text{-aqua})}$] and thus, the rate of the second-order reaction producing $[Mo_2(Cp)_2(\mu\text{-}SMe)_3(H_2O)(L)]^+$ (Scheme 3, step B). This is shown by the fact that **6**$^+$ was obtained more rapidly when **2** was treated with $HBF_4/Et_2O$ instead of $HBF_4/H_2O$. The effect of the nucleophile can be demonstrated by the fact that $[Mo_2(Cp)_2(\mu\text{-}SMe)_3L_2]^+$ (L = MeCN, *t*BuNC) was obtained "instantly" when a THF solution of **2** was treated by $HBF_4/H_2O$ in the presence of L, while **6**$^+$ (L = $H_2O$ or THF) was formed slowly upon treatment of **2** with $HBF_4/H_2O$ in THF in the absence of MeCN or *t*BuNC, even though the former reaction involves a supplementary step (substitution of $H_2O$ by a second L molecule) with respect to the latter. Substrate binding to the metal center, consecutive to (or concerted with) the cleavage of one Mo−O bond of the μ-aqua intermediate, was faster when L= MeCN or *t*BuNC than when L = $H_2O$ or THF. The formation of **2**$^+$ observed in the latter situation could arise by loss of a hydrogen atom from the μ-aqua intermediate (Scheme 3, step C). The fate of the hydrogen atom is not known.[28]

### *Electrochemical Oxidation of [Mo₂(Cp)₂(μ-SMe)₃(μ-OH)], 2. Reactivity of 2⁺*

With either THF or $CH_2Cl_2$ as solvent, complex **2** undergoes two oxidation steps; for both, the anodic-to-cathodic peak separation ($\Delta E_p$[20]) is smaller in $CH_2Cl_2$ than it is in THF (Table 1, Figure 1, a). Comparison of the first oxidation peak current [$(i_p{}^a)^{ox1}$][20] for equimolar $CH_2Cl_2$ solutions of **2** and of $[Mo_2(Cp)_2(\mu\text{-}SMe)_3(\mu\text{-}Cl)]$ (which undergoes a reversible one-electron oxidation in this solvent[4]) indicates that the first oxidation of **2** at ca −0.6 V involves one electron on the CV timescale.[29]

The current of the second oxidation of **2** ($E_{1/2}{}^{ox2} = -0.34$ V in THF, −0.15 V in $CH_2Cl_2$) is lower than that of the first step in both solvents [$i_p{}^{ox2}/i_p{}^{ox1} = 0.6$ (average) in THF]. The second oxidation of **2** is quasi-reversible,[21] the large peak-to-peak separation [in THF: $\Delta E_p$ = 330 mV (average) at 0.2 V·s$^{-1}$][20] suggesting that a chemical reaction takes place along with the electron-transfer. The small value of the rate constant of the heterogeneous electron-transfer ($k_e$ ca 6·10$^{-4}$ cm·s$^{-1}$ as estimated from CV simulations[40]) could indicate substantial structural reorganization without compositional change of the complex. Alternatively, a concerted reaction involving solvent-binding in THF is possible, since the potential and the CV peak separation of the second oxidation step are substantially affected by the nature of the solvent (Table 1). The dication cannot, however,

  

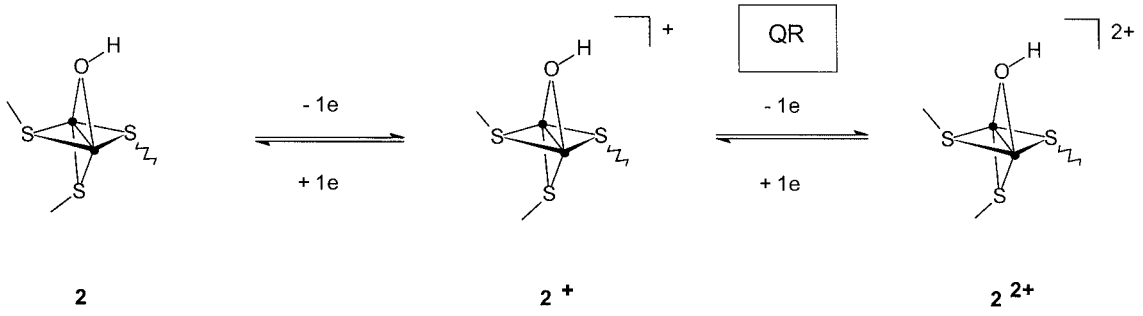


Scheme 4. • = Mo(Cp); QR = quasi-reversible electron-transfer

be isolated. The nature of the chemical step thus remains speculative and $2^{2+}$ will therefore be represented formally with a bridging hydroxide group in Scheme 4 and in the rest of the paper.

The reduction peak of **2** was not altered by tosylate, thereby demonstrating that **2** and $TsO^-$ do not react. In contrast, the oxidative part of the CV of **2** in THF was strongly affected by the presence of tosylate (Figure 1, b). Indeed, the second oxidation of **2** was not detectable when $TsO^-$ was present. Key features of the oxidation of **2** in the presence of $TsO^-$ include the detection of the two oxidation systems of **4** and of the reduction of the oxo complex $\mathbf{1}^+$ on the reverse scan (Figure 1, b and c). A rationalization of these features in terms of a reaction between $TsO^-$ and electrogenerated $\mathbf{2}^+$ is presented in Scheme 5.

This has been checked independently by treating a THF solution of $\mathbf{2}^+$ electrogenerated from $\mathbf{1}^+$ in the presence of 1 equivalent of $HBF_4/H_2O$ [see below and Figures 4(a) and 6(b)] with different substrates (MeCN, *t*BuNC, $CF_3CO_2^-$, $TsO^-$). The expected products, $[Mo_2Cp)_2(\mu\text{-}SMe)_3(L)_2]^+$ (L = MeCN, *t*BuNC), **3** and **4**, respectively, were obtained along with $\mathbf{1}^+$ in a ratio close to 1:1. The equilibrium in Scheme 5, formally a hydrogen atom transfer, probably arises from the deprotonation of $\mathbf{2}^+$, see below. Consistent with this, the CV of **2** in the presence of an excess of $CF_3CO_2^-$ in THF shows that the first one-electron oxidation of **2** is replaced by a reversible two-electron transfer at around −0.7 V. This is indicative of the $EC_{rev}E$ mechanism[21] shown in Scheme 6. Deprotonation of $\mathbf{2}^+$ by $CF_3CO_2^-$ produces the reduced oxo complex **1** which is oxidized at a potential more negative than that of **2** (ECE mechanism). The reversibility of the intervening chemical reaction (see below for the reduction of $\mathbf{1}^+$ in the presence of $CF_3CO_2H$) confers reversibility on the redox process and ensures that its potential is intermediate between those of $\mathbf{2}/\mathbf{2}^+$ and $\mathbf{1}/\mathbf{1}^+$.

Complex $\mathbf{2}^+$ could also be protonated. Addition of 1 equivalent of HTsO to a THF solution of $\mathbf{2}^+$ produced $\mathbf{4}^+$ (Figure 4). Similarly, treatment of $\mathbf{2}^+$ with $HBF_4/H_2O$ led to $\mathbf{6}^{2+}$. These results demonstrate that $\mathbf{2}^+$ can behave both as an acid and as a base.

### 2. Reduction of $[Mo_2(Cp)_2(\mu\text{-}SMe)_3(\mu\text{-}O)]^+$ ($\mathbf{1}^+$)

#### *In the Absence of Acid*

Complex $\mathbf{1}^+$ undergoes an irreversible oxidation and two reduction steps in $CH_2Cl_2$-, THF-, or MeCN/$NBu_4PF_6$ (Figure 5, a). The irreversible reduction around $E_p^{red} = -1.9$ V and the irreversible oxidation were not investigated. The potential of the first reduction is essentially independent of the solvent (Table 1). From the usual diagnostic criteria ($i_p^{red1}/v^{1/2}$ independent of scan rate, $v$; $(i_p^a/i_p^c)^{red1}$ close

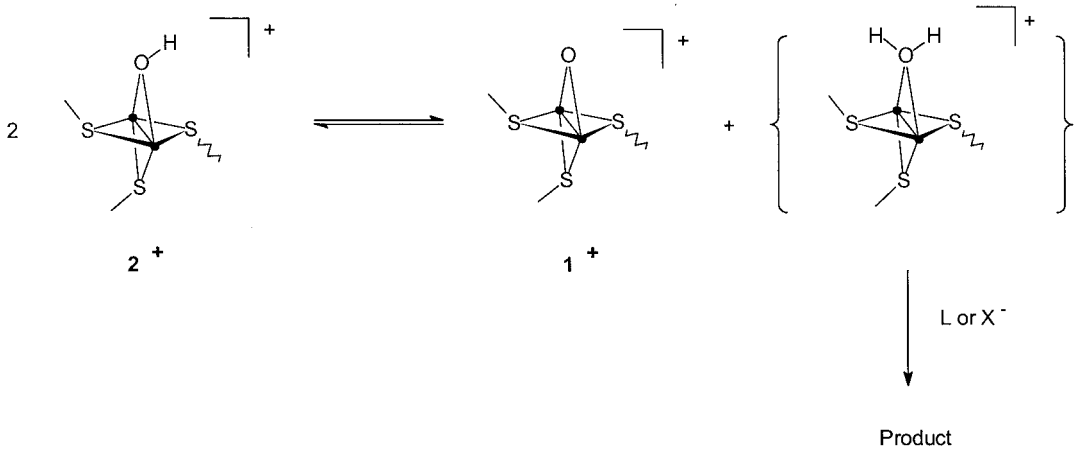


Scheme 5. • = Mo(Cp); methyl groups on the bridging S atoms are omitted

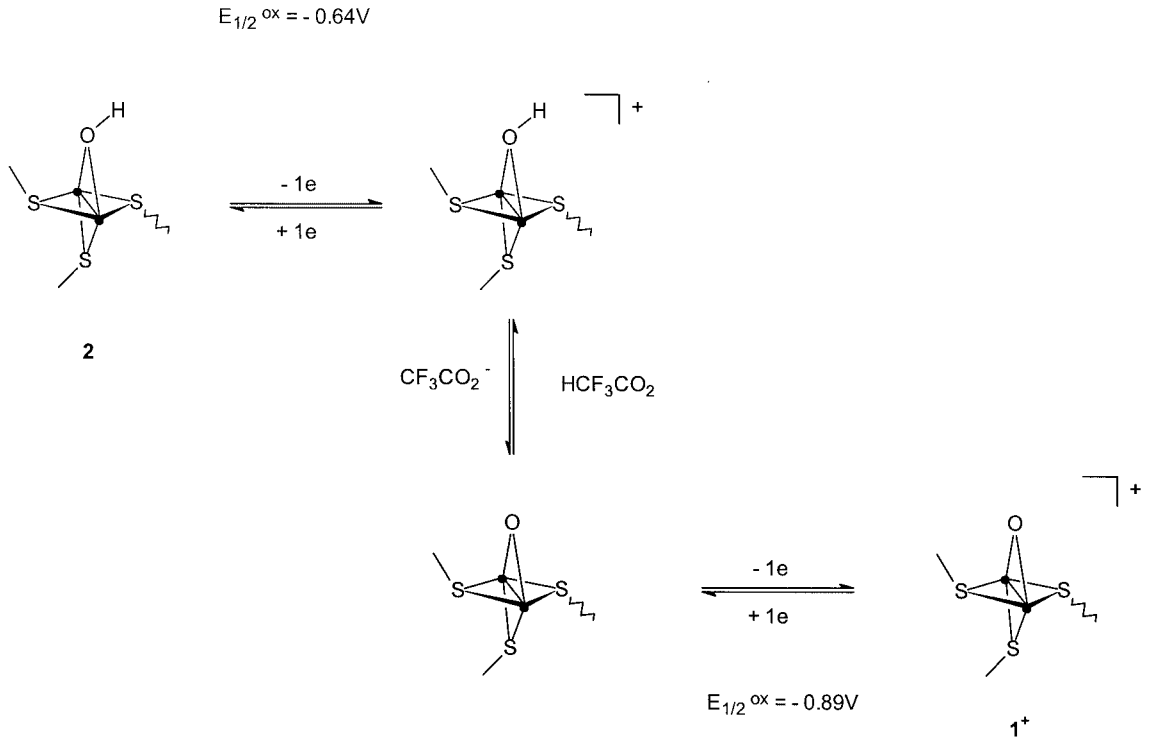


Scheme 6. • = Mo(Cp); methyl groups on the bridging S atoms are omitted

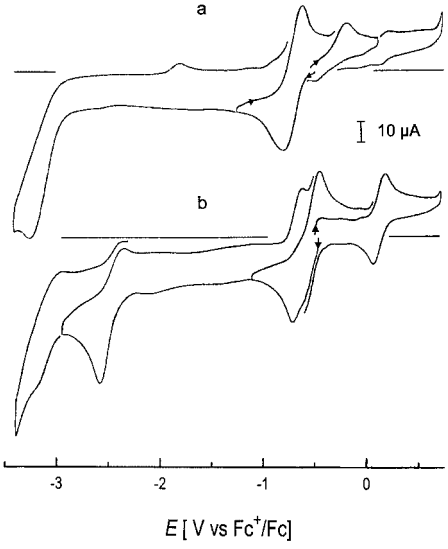


Figure 4. a) Cyclic voltammetry of $[Mo_2(Cp)_2(\mu\text{-}SMe)_3(\mu\text{-}OH)]^+$ ($\mathbf{2}^+$) generated by controlled-potential reduction ($n$ = 1 F·mol$^{-1}$ $\mathbf{1}^+$) of $\mathbf{1}^+$ (ca. 1.2 mM) in the presence of 1 equiv. $HBF_4/H_2O$; b) after addition of 1 equiv. HTsO to the solution in a). (THF/$NBu_4PF_6$; vitreous carbon electrode; scan rate $v$ = 0.2 V·s$^{-1}$)

vations have been made in the case of mononuclear imide and oxo complexes with the {Mo(dppe)$_2$} core.[30,31]

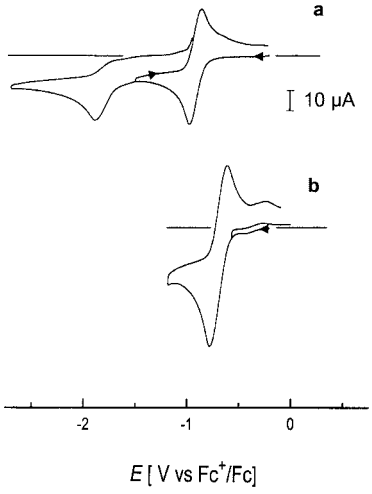


Figure 5. Cyclic voltammetry of $[Mo_2(Cp)_2(\mu\text{-}SMe)_3(\mu\text{-}O)]^+$ ($\mathbf{1}^+$) (ca. 1.5 mM) a) in the absence, and b) in the presence of 1 equivalent of $HBF_4/H_2O$ (THF/$NBu_4PF_6$; vitreous carbon electrode; scan rate $v$ = 0.2 V·s$^{-1}$).

to 1; $\Delta E_p$ ca 80mV),[21] the first reduction can be assigned to a reversible one-electron, diffusion-controlled step on the cyclic voltammetry timescale. The neutral oxo complex **1** is thus longer-lived than the isoelectronic imido derivative, since the reduction of $[Mo_2(Cp)_2(\mu\text{-}SMe)_3(\mu\text{-}NH)]^+$ was irreversible under the same conditions.[6] Similar obser-

Controlled-potential reduction of $\mathbf{1}^+$ in $CH_2Cl_2$/$NBu_4PF_6$ ($E_{el}$ = −1.0 V, Pt cathode, $n$ = 0.9 F·mol$^{-1}$ $\mathbf{1}^+$ by coulometry) afforded **1** in essentially quantitative yield,[18] as shown by cyclic voltammetry of the catholyte. In contrast, **1** was not obtained in a THF electrolyte. Under these conditions electrolysis of $\mathbf{1}^+$ (ca. 1 F·mol$^{-1}$ $\mathbf{1}^+$) afforded a product showing irreversible reduction and oxi-

  

dation processes ($E_p^{red} = -1.92$ V; $E_p^{ox} = -0.30$ V) which we have not attempted to characterize.

### *Reduction of 1⁺ in the Presence of Acid*

The products of controlled-potential electrolyses of **1**$^+$ performed in THF and in MeCN electrolytes in the presence of acid ($CF_3CO_2H$, HTsO, $HBF_4/H_2O$) were the same as those obtained by protonation of **2** (Scheme 1). This suggested that **2** might be an intermediate in the reduction of **1**$^+$ in acidic media. However, when HTsO (in THF) or $HBF_4/H_2O$ (in THF or in MeCN) were used, the same products as in Scheme 1 could also be obtained by controlled-potential reduction of **1**$^+$ at a potential where **2** could not be generated. The formation of these products by different pathways prompted us into a detailed investigation of the reduction mechanisms of **1**$^+$ in the presence of acid.

Addition of small amounts of $HBF_4/H_2O$ ($\leq 1$ equiv.) to a solution of **1**$^+$ in THF/$NBu_4PF_6$ resulted in the presence of a new reversible reduction around $-0.7$ V. The corresponding current increased with increasing acid concentration. Comparison of the peak current of **1**$^+$ in the absence of acid (Figure 5, a) to that of the reversible system at $E_{1/2}^{red} = -0.7$ V in the presence of 1 equivalent of acid (Figure 5, b) showed that two electrons are involved in the latter reduction. This arises from the observation that complex **1** generated at the electrode is protonated to **2**$^+$, which is reducible at a less negative potential than **1**$^+$ (ECE process). The reversibility of the observed (overall) two-electron reduction and the intermediate position of its potential relative to those of the **1**$^+$/**1** and **2**$^+$/**2** couples indicates that the chemical step (protonation of **1**) is reversible and that an $EC_{rev}E$ mechanism is operative (Scheme 7, path B). In agreement with Scheme 7, compound **2**$^+$ can be generated almost quantitatively[18] by controlled-potential reduction of **1**$^+$ in the presence of 1 equivalent of $HBF_4/H_2O$ (THF/$NBu_4PF_6$; $E_{el} = -0.9$ V; Pt or graphite cathode, electrolysis interrupted after the passage of 1 F mol$^{-1}$ **1**$^+$) (Figure 6, b).

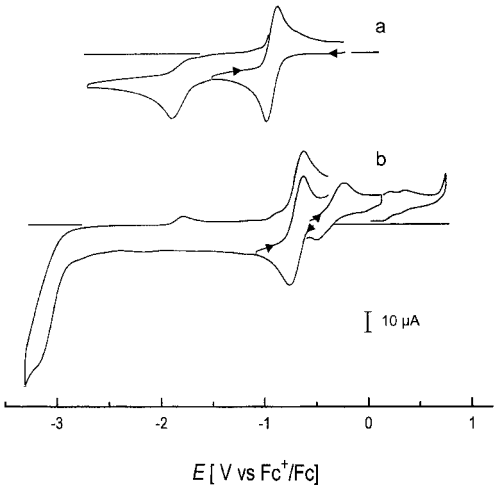


Figure 6. Cyclic voltammetry of $[Mo_2(Cp)_2(\mu\text{-}SMe)_3(\mu\text{-}O)]^+$ (**1**$^+$) (ca. 1.5 mM) a) before and b) after controlled-potential reduction ($E_{el} = -0.9$ V; $n = 1$ F·mol$^{-1}$ **1**$^+$) in the presence of 1 equivalent of $HBF_4/H_2O$ (see the solution in Figure 5,b) (THF/$NBu_4PF_6$; vitreous carbon electrode; scan rate $v = 0.2$ V·s$^{-1}$).

Further additions of $HBF_4/H_2O$ ($> 1$ equiv.) to a THF solution of **1**$^+$ led to the increase of the quasi-reversible reduction of **2**$^{2+}$ at $E_{1/2}^{red} = -0.34$ V while the reversible couple was slightly suppressed (Figure 7). These obser-

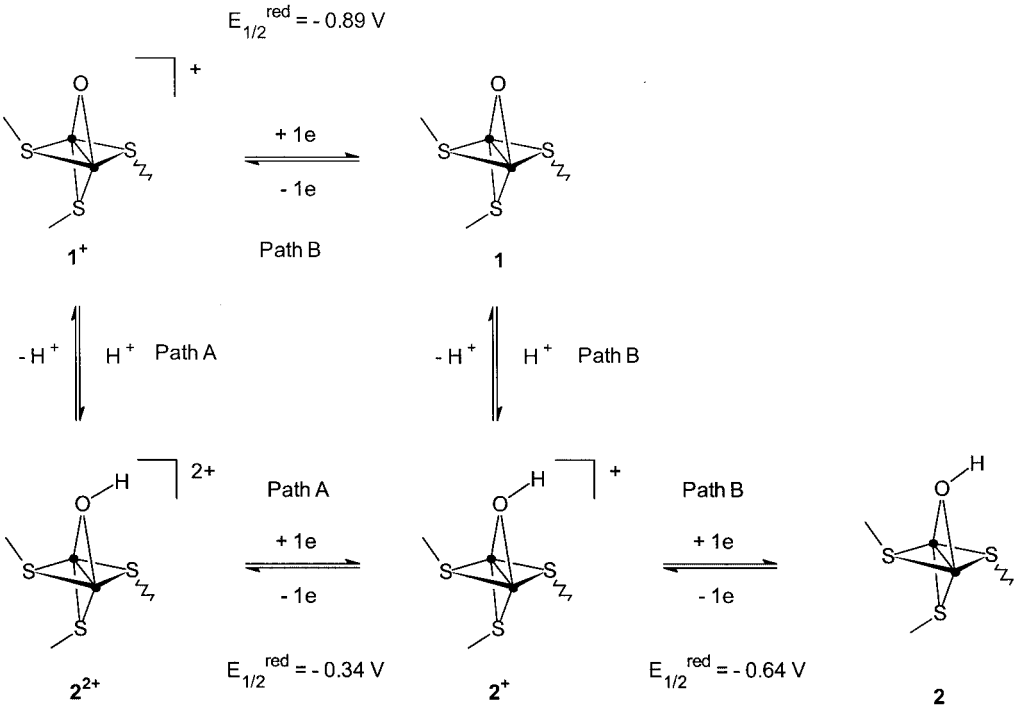


Scheme 7. • = Mo(Cp); methyl groups on the bridging S atoms are omitted

vations demonstrate that $\mathbf{1}^+$ can be protonated by $HBF_4/H_2O$ in THF (Scheme 7, path A), which is reminiscent of the behavior of the imide analogue of $\mathbf{1}^+$ in acidic media, since protonation of the imide cation to the amide dication was also observed.[6] The protonation of $\mathbf{1}^+$ is reversible, since it is still possible to detect the irreversible oxidation of $\mathbf{1}^+$ in the presence of acid, with little modification of the corresponding peak current. The first steps of the reduction mechanism of $\mathbf{1}^+$ in the presence of $HBF_4/H_2O$ are presented in Scheme 7. We believe that the reactions of $\mathbf{2}^+$ with substrates, which are depicted as hydrogen atom transfers in Scheme 5, actually arise from the acid-base equilibrium in Scheme 7, path B. Complex **1** formed by deprotonation of $\mathbf{2}^+$ would be oxidized by $\mathbf{2}^+$ in a homogeneous redox reaction ($E_{1/2}^{red}$ $\mathbf{2}^+ = -0.64$ V; $E_{1/2}^{ox}$ **1** $= -0.89$ V) producing **2** and $\mathbf{1}^+$. Protonation of **2** would then afford the μ-aqua intermediate (Scheme 8). The overall reaction in Scheme 8 is equivalent to the equilibrium in Scheme 5.

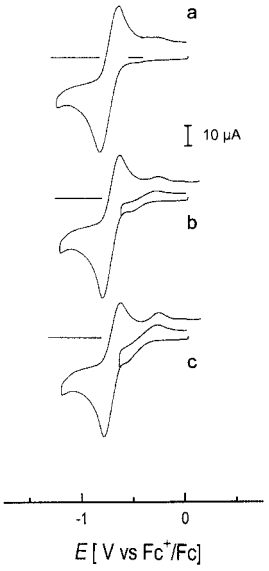


Figure 7. Cyclic voltammetry of $[Mo_2(Cp)_2(\mu\text{-}SMe)_3(\mu\text{-}O)]^+$ ($\mathbf{1}^+$) (ca. 1.4 mM) in the presence of a) 1 equivalent, b) 2 equivalents, and c) 3 equivalents of $HBF_4/H_2O$ (THF/$NBu_4PF_6$; vitreous carbon electrode; scan rate $v = 0.2$ V·s$^{-1}$).

In addition to the increase of the $\mathbf{2}^{2+}/\mathbf{2}^+$ quasi-reversible reduction, addition of acid (> 2 equiv. $HBF_4/H_2O$) causes a gradual loss of reversibility of the two-electron reduction around −0.7 V, with $(i_p^a/i_p^c) < 1$ at slow scan rates. This shows the occurrence after the $EC_{rev}E$ mechanism of other chemical step(s) which eventually lead to $\mathbf{6}^+$. Controlled-potential electrolysis of $\mathbf{1}^+$ performed at −0.9 V (Pt cathode; $n = 2.2\pm0.2$ F·mol$^{-1}$ $\mathbf{1}^+$ [32]) in the presence of an excess (> 3 equiv.) of $HBF_4/H_2O$ effectively produces $\mathbf{6}^+$, characterized by two one-electron oxidation steps and by an irreversible reduction (Table 1). Electrolyses carried out at −0.5 V, a potential which does not permit the reduction of $\mathbf{2}^+$, also produced $\mathbf{6}^+$ after transfer of ca 2 F·mol$^{-1}$ $\mathbf{1}^+$.[32] Under the latter conditions the formation of $\mathbf{6}^+$ occurs exclusively via reduction of $\mathbf{2}^{2+}$ and subsequent protonation of $\mathbf{2}^+$ (Schemes 7 and 9, path A). We have checked, in separate experiments, that addition of $HBF_4/H_2O$ to a solution of $\mathbf{2}^+$ effectively produces $\mathbf{6}^{2+}$. The different mechanisms leading to the formation of the product, $\mathbf{6}^+$, are described by Schemes 7 and 9.

We have already mentioned that oxidation of $\mathbf{6}^+$ occurs according to an $EC_{rev}$ process where the chemical step is a proton transfer. This protonation equilibrium (between $\mathbf{2}^+$

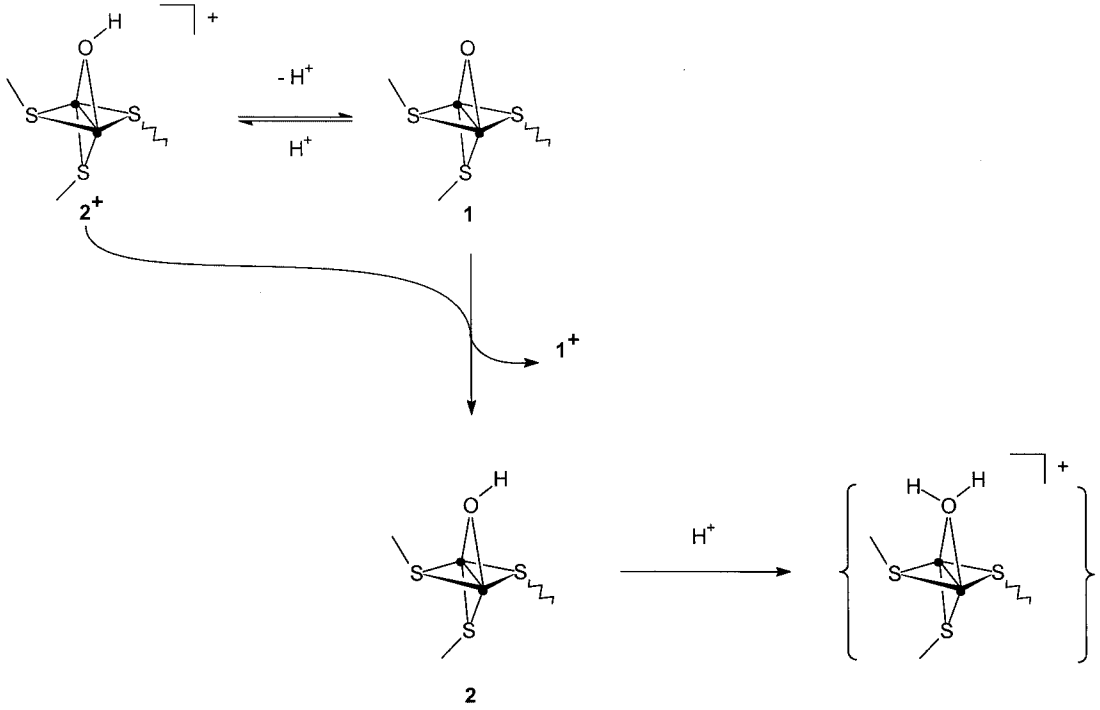


Scheme 8. • = Mo(Cp); methyl groups on the bridging S atoms are omitted

  

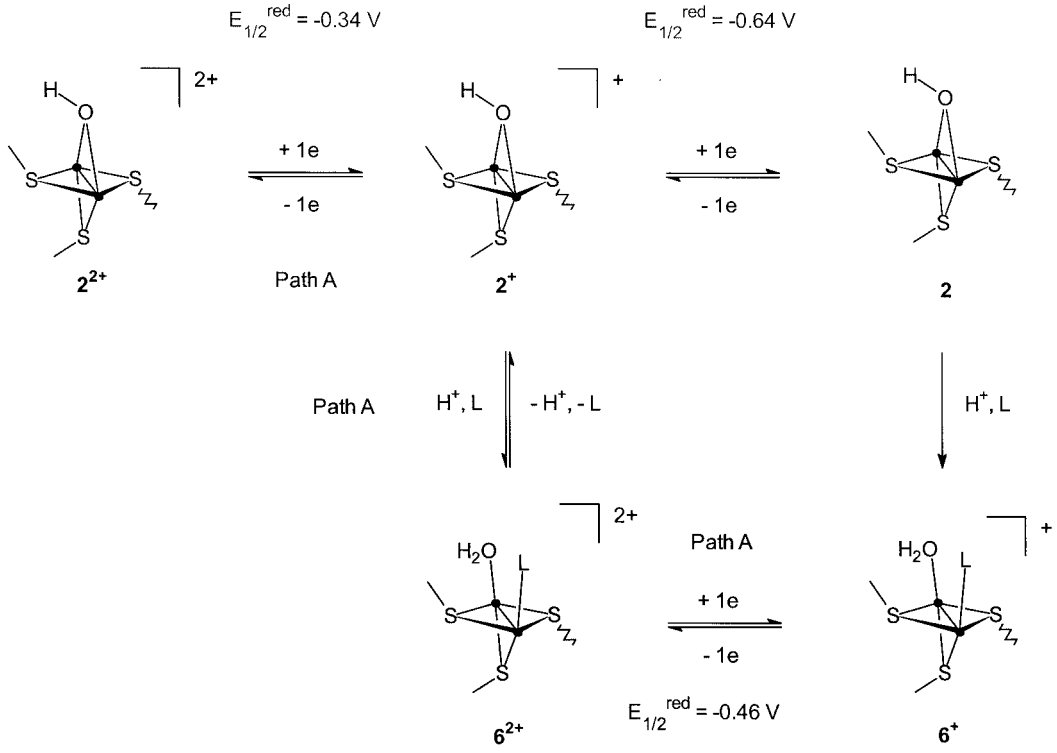


Scheme 9. • = Mo(Cp); methyl groups on the bridging S atoms are omitted

and $\mathbf{6}^{2+}$) is entirely consistent with the results of the electrochemical study of the reduction of $\mathbf{1}^{+}$ in the presence of $HBF_4$ (Scheme 9).

The electrochemical reduction of $\mathbf{1}^{+}$ in the presence of $HBF_4/H_2O$ in MeCN follows the same type of mechanism as in THF (Schemes 7 and 9), except that the products $\mathbf{6}^{2+}$ and $\mathbf{6}^{+}$ are replaced by $\mathbf{5}^{2+}$ and $\mathbf{5}^{+}$, respectively.

In the presence of trifluoroacetic acid (2 equiv.; THF/$NBu_4PF_6$), the CV of $\mathbf{1}^{+}$ also shows a reversible overall two-electron reduction with $E_{1/2}^{red} = -0.72$ V, indicative of an $EC_{rev}E$ mechanism (see Scheme 6, Figure 8, a). The decrease of the anodic-to-cathodic peak current ratio $[(i_p^a/i_p^c)^{red}]$ with decreasing scan rates demonstrates that the $EC_{rev}E$ process is followed by one or more further chemical steps. Consistent with this observation, two reversible one-electron oxidations were detected at $E_{1/2}^{ox1} = -0.35$ V (Figure 8, a) and $E_{1/2}^{ox2} = 0.35$ V (not shown on Figure 8, a) on the reverse scan. These are due to $[Mo_2(Cp)_2(\mu\text{-}SMe)_3(\mu\text{-}\eta^1,\eta^1\text{-}OCOCF_3)]$ (**3**) as is evident by comparison with the redox potentials of an authentic sample of this complex. Controlled-potential electrolysis performed under these conditions at the potential of the reduction step (Pt cathode, 1.6 F·mol$^{-1}$ $\mathbf{1}^{+}$) produced **3** almost quantitatively[18] (Figure 8, b). The nature of the product was confirmed by comparison of the $^1H$ and $^{19}F$ NMR spectra of the solid isolated from the catholyte to those of an authentic sample of **3** prepared independently and characterized crystallographically (see below).

The reduction of $\mathbf{1}^{+}$ in the presence of HTsO was also investigated. Addition of 1 equivalent of acid resulted in the

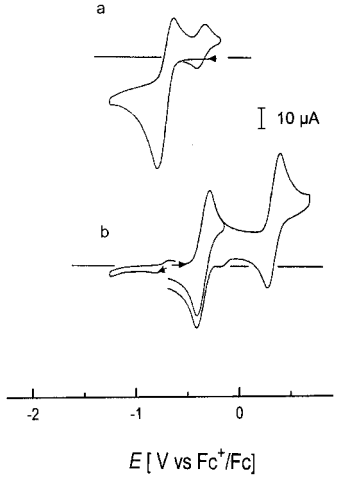


Figure 8. Cyclic voltammetry of $[Mo_2(Cp)_2(\mu\text{-}SMe)_3(\mu\text{-}O)]^{+}$ ($\mathbf{1}^{+}$) (ca. 1.4 mM) in the presence of 2 equivalents $CF_3CO_2H$ a) before, and b) after controlled-potential reduction at −0.95 V (1.6 F·mol$^{-1}$ $\mathbf{1}^{+}$) (THF/$NBu_4PF_6$; vitreous carbon electrode; scan rate $v = 0.2$ V·s$^{-1}$)

presence of a reduction peak at −0.68 V. Comparison of the corresponding current with that of $\mathbf{1}^{+}$ in the absence of acid indicated that more than one electron is involved in the process. In contrast with the CV recorded in the presence of 1 equivalent of $HBF_4/H_2O$ or $CF_3CO_2H$, the reduction is not fully reversible $[(i_p^a/i_p^c) < 1]$ and the redox systems of **4** were detected on the return scan. This is again consistent with an initial $EC_{rev}E$ mechanism, but in this case the prod-

  

uct-forming reaction subsequent to the electrochemical process is faster than in previous examples. This might be due to two factors: (i) formation of the product requires less rearrangement for **4** than it does, for example, for **3** and (ii) formation of **4** is faster than that of $\mathbf{6}^+$ due to either a concerted attack of HTsO on **2** (and/or $\mathbf{2}^+$) or to a faster binding to the μ-aqua intermediate (see above) of $TsO^-$ compared with L (L = $H_2O$ or THF).

Controlled-potential electrolysis of $\mathbf{1}^+$ in the presence of 2 equivalents of HTsO produced **4** quantitatively[18] after transfer of ca 2 $F\cdot mol^{-1}$ $\mathbf{1}^+$. Since protonation of $\mathbf{2}^+$ by HTsO afforded $\mathbf{4}^+$ (Figure 4), two different pathways (similar to paths A and B in Scheme 9) can be followed. Evidence for the formation of $\mathbf{4}^+$ was obtained by voltammetry at the rotating disc electrode of the catholyte after the electrolysis was interrupted after passage of 1 $F\cdot mol^{-1}$ $\mathbf{1}^+$: this showed the presence of both **4** and $\mathbf{4}^+$ in the solution.

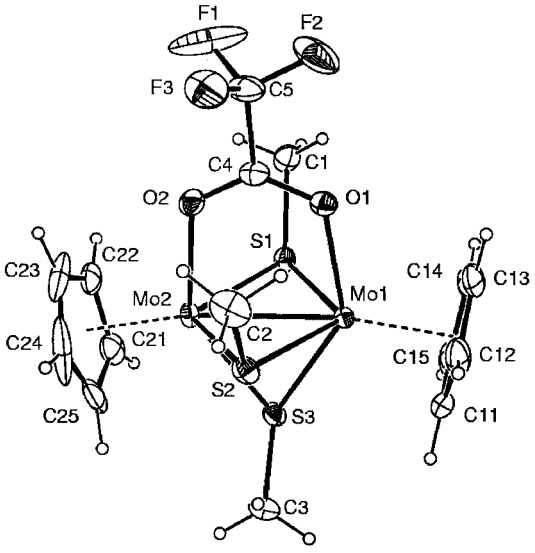


Figure 9. The molecular structure of $[Mo_2(cp)_2(\mu\text{-}SMe)_3(\mu\text{-}\eta^1,\eta^1\text{-}OCOCF_3)]$ (**3**) showing 20% ellipsoids

### Solid State Structure of $[Mo_2(Cp)_2(\mu\text{-}SMe)_3(\mu\text{-}\eta^1,\eta^1\text{-}OCOCF_3)]$ (3)

The results of a single-crystal X-ray diffraction study of **3** (Figure 9, Table 2) confirmed the molecular structure proposed on the basis of the spectroscopic and analytical data presented in the Experim. Section. In particular, they demonstrate that the μ-hydroxo ligand in **2** has been replaced by a bridging trifluoroacetate group in **3**.

In the structure of **3** the two molybdenum atoms [Mo−Mo = 2.709(1) Å] are linked by four bridging ligands: three methylthiolates and a trifluoroacetate group. Each metal atom thereby attains a four-legged piano-stool coordination. This dinuclear structure is of a novel type in as much as that structurally characterized μ-carboxylato−$Mo_2^{III}$ species are usually triply-bridged compounds with long Mo−Mo bonds e.g. in $[\{Mo_2(NC_6H_4CH_3)(S_2POEt_2)\}_2(\mu\text{-}S)(\mu\text{-}SR)(\mu\text{-}O_2CCF_3)]$ (R = H, Me),[33] and $[L_2Mo_2(\mu\text{-}O)(\mu\text{-}O_2CCH_3)_2]^{2+}$ (L = *N*,*N*′,*N*′′-trimethyl-1,4,7-triazacyclononane)[34] the Mo−Mo distances are 2.839(2), 2.844(1), and 2.885(1) Å, respectively. The Mo−Mo bond in the quadruply-bridged dinuclear molybdenum(IV) complex $[(Cp^*Mo)_2(\mu\text{-}O_2CMe)_2(\mu\text{-}PMe_2)(\mu\text{-}CH_3)]$ [Mo−Mo = 2.845(1) Å][35] is also significantly longer than that in **3**. However, Poli et al. recently reported a short Mo−Mo bond of 2.553(1) Å in the quadruply-bridged molybdenum(IV) complex $[(Cp^*Mo)_2(\mu\text{-}O)_2(\mu\text{-}O_2CMe)_2]$;[36] this contrasts with the long Mo−Mo bond [2.799(4) Å] found in the related triply-bridged molybdenum(IV) compound $[(Cp^*MoCl)_2(\mu\text{-}O)(\mu\text{-}Cl)(\mu\text{-}O_2COH)]$.[37] Metal−metal bonds in comparable thiolato-bridged bimetallic anions $[\{Mo(CO)_3\}_2(\mu\text{-}SR)_2(\mu\text{-}O_2CR')]^-$ {R = $C_6H_5$, *p*-$ClC_6H_4$; R′ = $CMe_3$, $CF_3$, $C(Me)=CH_2$}[38] where the molybdenum atoms are in low oxidation states (e.g. I) are much longer (ca. 2.91 Å) than that in **3**. It is clear, then, that the oxidation states of the metal atoms and the number and size of the bridging groups all play a part in bringing about the large variations

Table 2. Selected distances (Å) and angles (deg.) for $[Mo_2(cp)_2(\mu\text{-}SMe)_3(\mu\text{-}\eta^1,\eta^1\text{-}OCOCF_3)]$ (**3**)

| | | | |
|---|---|---|---|
| Mo(1)−Mo(2) | 2.709(1) | Mo(2)−O(2) | 2.173(3) |
| Mo(1)−O(1) | 2.174(3) | Mo(2)−S(1) | 2.443(1) |
| Mo(1)−S(1) | 2.430(1) | Mo(2)−S(2) | 2.447(1) |
| Mo(1)−S(2) | 2.446(1) | Mo(2)−S(3) | 2.421(1) |
| Mo(1)−S(3) | 2.429(1) | O(2)−C(4) | 1.245(5) |
| O(1)−C(4) | 1.258(5) | C(4)−C(5) | 1.533(6) |
| | | | |
| Mo(2)−S(1)−Mo(1) | 67.5(1) | O(2)−Mo(2)−Mo(1) | 83.9(1) |
| Mo(2)−S(2)−Mo(1) | 67.2(1) | O(2)−Mo(2)−S(1) | 85.3(1) |
| Mo(2)−S(3)−Mo(1) | 67.9(1) | O(2)−Mo(2)−S(2) | 84.2(1) |
| O(1)−Mo(1)−Mo(2) | 84.0(1) | O(2)−Mo(2)−S(3) | 140.0(1) |
| O(1)−Mo(1)−S(1) | 85.6(1) | C(4)−O(1)−Mo(1) | 121.8(3) |
| O(1)−Mo(1)−S(2) | 84.0(1) | C(5)−O(2)−Mo(2) | 122.3(2) |
| O(1)−Mo(1)−S(3) | 139.9(1) | O(1)−C(4)−O(2) | 128.0(4) |
| O(1)−C(4)−C(5) | 116.5(4) | O(2)−C(4)−C(5) | 115.5(4) |
| | | | |
| O(1)−Mo(1)−Mo(2)−O(2) | 0.2(1) | O(1)−Mo(1)−Mo(2)−S(3) | 178.5(1) |
| O(1)−Mo(1)−Mo(2)−S(2) | −86.8(1) | O(1)−Mo(1)−Mo(2)−S(1) | 88.7(1) |

  

in the Mo-Mo distances found in these μ-carboxylato complexes.[33,38]

The mean Mo−S bond length in **3** (2.436 Å) is comparable with values for other acetato−thiolato-bridged compounds, such as $[\{Mo_2(NC_6H_4CH_3)(S_2POEt_2)\}_2(\mu\text{-}S)(\mu\text{-}SR)(\mu\text{-}O_2CCF_3)]$,[33] and $[\{Mo(CO)_3\}_2(\mu\text{-}SR)_2(\mu\text{-}O_2CR')]^-$[38] (average 2.456 Å). However, the shorter Mo−Mo bond in **3** requires the Mo−S−Mo angles to be more acute (average 67.5°) than those in the above mentioned compounds (average 72.0°).[33,38] The structural features of the $CF_3CO_2$ ligand, in particular the nearly equal C(4)−O(1) and C(4)−O(2) bond lengths of 1.258(5) and 1.245(5) Å, are unexceptional[33−38] and indicate π-electron delocalization over the O(1), O(2), and C(4) atoms. The Mo−O distances of 2.174(3) and 2.173(3) Å indicate single bonds. They are significantly shorter than values in neutral, triply-bridged dimolybdenum(III) complexes with acetate ligands (average 2.267 Å),[33] but are close to those in neutral, quadruply-bridged dimolybdenum(IV) compounds (average 2.161 Å).[36]

The heavy atom skeleton of **3**, excluding C3 and F1−F3, has approximate mirror symmetry: none of the nine atoms Mo1, Mo2, S3, O1, O2, C4, C5, C13, and C23 lie more than 0.04 Å from their common plane.

## Conclusion

This work has illustrated the reactivity both of bridging oxo and hydroxo ligands in acidic media and of aqua ligands. It leads to four main conclusions.

**(A)** We have shown that protonation at a μ-OH ligand in a dimolybdenum complex is possible. Depending on the conditions (nature of the conjugate base, presence of a π-acid ligand L), the product can either retain the protonated OH bridge as a terminally bonded $H_2O$ ligand or give rise to a disubstituted complex after elimination of a water molecule. It follows that protonation of $[Mo_2(Cp)_2(\mu\text{-}SMe)_3(\mu\text{-}OH)]$ gives ready access to one or more coordination sites at the metal centers.

**(B)** The reactivity of $\mathbf{2}^+$, due to its amphoteric nature, is also quite rich. Protonation of $\mathbf{2}^+$ by HTsO or $HBF_4/H_2O$ in THF produces $\mathbf{4}^+$ or $\mathbf{6}^{2+}$, respectively. On the other hand, the products obtained on addition of $CF_3CO_2H$ to $\mathbf{2}^+$, that is $\mathbf{1}^+$ and **3**, result from the reaction of the trifluoroacetate anion with the μ-aqua complex (see Scheme 5), rather than from protonation of the μ-hydroxo cation. The equilibrium in Scheme 5, which is formally a hydrogen atom transfer, could result from an acid-base equilibrium between $\mathbf{2}^+$ and **1**, coupled to a redox reaction between these species (Scheme 8).

**(C)** Both the oxo cation, $\mathbf{1}^+$, and its reduced form, **1**, can be protonated. The difference in $pK_a$ between the $\mathbf{2}^{2+}$ and $\mathbf{2}^+$ forms can be estimated from the thermochemical cycle in Scheme 7. This $\Delta pK_a$ value, which is approximate because of the quasi-reversible nature of the $\mathbf{2}^{2+}/\mathbf{2}^+$ couple, is around 11 units in MeCN [$E_{1/2}(\mathbf{2}^{2+}/\mathbf{2}^+) = -0.24$ V; $E_{1/2}(\mathbf{1}^+/\mathbf{1}) = -0.89$ V] and about 9 units in THF [$E_{1/2}(\mathbf{2}^{2+}/\mathbf{2}^+) = -0.34$ V; $E_{1/2}(\mathbf{1}^+/\mathbf{1}) = -0.89$ V]. Similarly, the $\Delta pK_a$ between the $\mathbf{2}^+$ and **2** forms can be estimated using the redox potentials of the $\mathbf{2}^+/\mathbf{2}$ and $\mathbf{1}/\mathbf{1}^-$ reduction steps; in this case, $\Delta pK_a$ is about 20 units. Although this figure is at best a rough estimate since the $\mathbf{1}/\mathbf{1}^-$ irreversible reduction is shifted from the thermodynamic potential, it nevertheless illustrates the dramatic effect of the metal core oxidation state on the acidity of the μ-OH proton.

Since $\mathbf{1}^+$ can be protonated by $HBF_4/H_2O$ to give $\mathbf{2}^{2+}$ it is possible to generate coordination sites (and access to $\mathbf{6}^+$ or products derived therefrom) at a potential ca 0.4 V less negative than would be required in the absence of such a protonation step. This conclusion is important for any consideration of biological processes involving redox enzymes since the range of potentials accessible to natural reductants is restricted.

**(D)** We have also shown that electrochemical reduction of a species containing a terminal aqua ligand leads to a hydroxo bridge (with elimination of a hydrogen atom). Oxidation of a compound containing terminally bonded water also affords a bridging hydroxide after the release of a proton. This kind of redox-induced reactivity at a terminal aqua ligand could also be relevant to different types of enzyme-driven reactions.

## Experimental Section

**Methods and Materials:** All the experiments were carried out under an inert atmosphere using Schlenk techniques for the syntheses. Tetrahydrofuran (THF) was purified as described previously.[6] Acetonitrile (Merck, HPLC grade) was used as received. The acids, *p*-toluenesulfonic (Prolabo), trifluoroacetic (Aldrich), fluoroboric (diethyl ether complex and aqueous solution, Aldrich), were used as received. The preparation and purification of the supporting electrolyte $NBu_4PF_6$ and the configuration of the electrochemical equipment were as described previously.[6] All the potentials (text, tables, figures) are quoted relative to the ferrocene−ferrocenium couple. Ferrocene was added as an internal standard at the end of the experiments. $^1H$ NMR spectra were recorded on a Bruker AC300 spectrometer. Shifts are relative to tetramethylsilane as an internal reference. Chemical analyses were carried out at the Centre de Microanalyses du CNRS, Vernaison. Complexes $[Mo_2(Cp)_2(\mu\text{-}SMe)_3(\mu\text{-}O)]^+$ ($\mathbf{1}^+$), $[Mo_2(Cp)_2(\mu\text{-}SMe)_3(\mu\text{-}OH)]$ (**2**), and $[Mo_2(Cp)_2(\mu\text{-}SMe)_3(L)_2]^+$ were synthesized as described previously.[4,10,19]

**Synthesis of $[Mo_2(Cp)_2(\mu\text{-}SMe)_3(\mu\text{-}\eta^1,\eta^1\text{-}OCOCF_3)]$ (3):** $[Mo_2(cp)_2(\mu\text{-}SMe)_3(MeCN)_2][BF_4]$ (100 mg, 0.158 mmol) and a 0.346 M solution (450 μL of) of $Et_4NCF_3CO_2/H_2O$ prepared by neutralization of a THF solution of $CF_3CO_2H$ by $Et_4NOH$ (40% in methanol) were added to THF (20 mL). After stirring for 5 minutes the dark red solution was evaporated to dryness. The residue was stirred with pentane (100 mL), the dark red solution was filtered, and pentane was evaporated under vacuum. After stirring in cold pentane and elimination of the solvent by filtration, the solid was vacuum dried. Yield 80 mg (0.139 mmol, 88%). C,H analysis for $C_{15}H_{19}O_2F_3S_3Mo_2$ (575.8): calcd. C, 31.3, H 3.3; found C 31.6, H 3.4. $^1H$ NMR, $(CD_3)_2CO$: δ = 5.36 (s, 10 H, $C_5H_5$), 1.53 (s, 3 H, $SCH_3$),1.38 (s, 3 H, $SCH_3$), 1.32 (s, 3 H, $SCH_3$). $^{19}F$ NMR $(CD_3)_2CO$: −73.9 ($CF_3CO_2$).

  

**X-ray Analysis:** Crystals of $[Mo_2(Cp)_2(\mu\text{-}SMe)_3(\mu\text{-}\eta^1,\eta^1\text{-}OCOCF_3)]$ (**3**) were obtained at room temperature from a pentane solution. Measurements were made with a plate-shaped crystal, 0.30 × 0.30 × 0.03 mm, on a Nonius CAD4 diffractometer with Mo-$K_\alpha$ X-rays, λ = 0.71073 Å. Intensities were estimated from ω/2θ scans and corrected empirically for absorption from ψ-scans (transmission factors 0.640−0.953). The structure was solved by Patterson methods and refined by full-matrix least-squares on $F^2$ using all independent reflections with $2\theta < 60°$.[39] Hydrogen atoms rode on their parent carbon atoms. A single orientation parameter was refined for each methyl group.

Crystal data for **3**, $C_{15}H_{19}F_3Mo_2O_2S_3$; $M$ = 576.36, monoclinic, space group $P2_1/c$, $a$ = 12.8796(5), $b$ = 9.0131(5), $c$ = 16.8558(5) Å, β = 91.411(3)°, $V$ = 1956.11(14) Å$^3$, $Z$ = 4, $T$ = 20 °C, $\rho_{calcd.}$ = 1.957 g cm$^{-3}$, μ(Mo-$K_\alpha$) = 1.636 mm$^{-1}$, $F$(000) = 1136, 7166 reflections collected, 5675 unique ($R_{int}$ = 0.0240), 229 parameters refined, $R1$ = 0.0705 and $wR(F^2)$ = 0.0903 over all 5675 data used in refinement. Extreme Δρ values: 0.79−0.67 e·Å$^{-3}$.

CCDC-216408 contains the supplementary crystallographic data for this paper. These data can be obtained free of charge via www.ccdc.cam.ac.uk/conts/retrieving.html or from the Cambridge Crystallographic Data Center, 12 Union Road, Cambridge CB2 1EZ, UK; Fax: + 44-1223-336-033; or E-mail: deposit@ccdc.cam.ac.uk.

## Acknowledgments

The authors thank the CNRS (France), the EPSRC (UK), Université de Bretagne Occidentale and Glasgow University for financial support. The Conseil Régional de Bretagne is acknowledged for financial support of this work (PRIR, Operation n° 98CCO9) and for providing a studentship to M. L. H.

[1] F. Y. Pétillon, P. Schollhammer, J. Talarmin, K. W. Muir, *Coord. Chem. Rev.* **1998**, *178−180*, 203−247.
[2] P. Madec, K. W. Muir, F. Y. Pétillon, R. Rumin, Y. Scaon, P. Schollhammer, J. Talarmin, *J. Chem. Soc., Dalton Trans.* **1999**, 2371−2383.
[3] P. Schollhammer, E. Guénin, F. Y. Pétillon, J. Talarmin, K. W. Muir, D. S. Yufit, *Organometallics* **1998**, *17*, 1922−1924.
[4] F. Barrière, Y. Le Mest, F. Y. Pétillon, S. Poder-Guillou, P. Schollhammer, J. Talarmin, *J. Chem. Soc., Dalton Trans.* **1996**, 3967−3976.
[5] F. Y. Pétillon, P. Schollhammer, J. Talarmin, *J. Chem. Soc., Dalton Trans.* **1997**, 4019−4024.
[6] J. Y. Cabon, C. Le Roy, K. W. Muir, F. Y. Pétillon, F. Quentel, P. Schollhammer, J. Talarmin, *Chem. Eur. J.* **2000**, *6*, 3033−3042.
[7] F. Y. Pétillon, P. Schollhammer, J. Talarmin, K. W. Muir, *Inorg. Chem.* **1999**, *38*, 1954−1955; N. Le Grand, K. W. Muir, F. Y. Pétillon, C. J. Pickett, P. Schollhammer, J. Talarmin, *Chem. Eur. J.* **2002**, *8*, 3115−3127.
[8] P. Schollhammer, N. Cabon, J. F. Capon, F. Y. Pétillon, J. Talarmin, K. W. Muir, *Organometallics* **2001**, *20*, 1230−1242.
[9] P. Schollhammer, M. Pichon, K. W. Muir, F. Y. Pétillon, R. Pichon, J. Talarmin, *Eur. J. Inorg. Chem.* **1999**, 221−223.
[10] P. Schollhammer, M. Le Hénanf, C. Le Roy-Le Floch, F. Y. Pétillon, J. Talarmin, K. W. Muir, *J. Chem. Soc., Dalton Trans.* **2001**, 1573−1577.
[11] S. J. Lippard, *Angew. Chem. Int. Ed. Engl.* **1988**, *27*, 344−361; D. M. Kurtz, Jr., *Chem. Rev.* **1990**, *90*, 585−606; R. Than, A. A. Feldmann, B. Krebs, *Coord. Chem. Rev.* **1999**, *182*, 211−241; E. I. Solomon, *Inorg. Chem.* **2001**, *40*, 3656−3669.
[12] M. N. Collomb Dunand-Sauthier, A. Deronzier, A. Piron, *J. Electroanal. Chem.* **1999**, *463*, 119−122; M. N. Collomb, A. Deronzier, A. Richardot, J. Pécaut, *New J. Chem.* **1999**, *23*, 351−353.
[13] T. Tanase, N. Takeshita, S. Yano, I. Kinoshita, A. Ichimura, *New J. Chem.* **1998**, 927−929; T. Tanase, N. Takeshita, C. Inoue, M. Kato, S. Yano, K. Sato, *J. Chem. Soc., Dalton Trans.* **2001**, 2293−2302.
[14] Y. Sasaki, M. Suzuki, A. Nagasawa, A. Tokiwa, M. Ebihara, T. Yamagushi, C. Kabuto, T. Ochi, T. Ito, *Inorg. Chem.* **1991**, *30*, 4903−4908; A. Kikuchi, T. Fukumoto, K. Umakoshi, Y. Sasaki, A. Ichimura, *J. Chem. Soc., Chem. Commun.* **1995**, 2125−2126; T. Fukumoto, A. Kikuchi, K. Umakoshi, Y. Sasaki, *Inorg. Chim. Acta* **1998**, *283*, 151−159.
[15] K. Wieghardt, U. Bossek, A. Neves, B. Nuber, J. Weiss, *Inorg. Chem.* **1989**, *28*, 432−440; K. Wieghardt, M. Guttmann, P. Chaudhuri, W. Gebert, M. Minelli, C. G. Young, J. H. Enemark, *Inorg. Chem.* **1985**, *24*, 3151−3155.
[16] V. R. Ott, F. A. Schultz, *J. Electroanal. Chem.* **1975**, *59*, 47−60; V. R. Ott, F. A. Schultz, *J. Electroanal. Chem.* **1975**, *61*, 81−98; V. R. Ott, D. S. Swieter, F. A. Schultz, *Inorg. Chem.* **1977**, *16*, 2538−2545.
[17] M. B. Gomes de Lima, J. E. Guerchais, R. Mercier, F. Y. Pétillon, *Organometallics* **1986**, *5*, 1952−1964.
[18] The yield of the reaction of **2** with different acids was calculated by comparing the peak current of the reactant with that of the product, assuming identical diffusion coefficients. Similar procedures were used to estimate the yield of controlled-potential electrolyses, or that of the reaction of **4** or **6**$^+$ with different substrates.
[19] N. Cabon, E. Paugam, F. Y. Pétillon, P. Schollhammer, J. Talarmin, K. W. Muir, *Organometallics* **2003**, *22*, 4178−4180.
[20] The parameters $i_p$ and $E_p$ are the peak current and the peak potential of a redox process, respectively; $E_{1/2} = (E_p^a + E_p^c)/2$; $E_p^a$, $i_p^a$ and $E_p^c$, $i_p^c$ are the potential and the current of the anodic and of the cathodic peak of a reversible process, respectively; $\Delta E_p = E_p^a - E_p^c$; $k_e$ (in cm/s) is the rate constant of the heterogeneous electron-transfer; an EC process comprises an electron-transfer step (E) followed by a chemical reaction (C). CV and CPE stand for cyclic voltammetry and controlled-potential electrolysis, respectively; $v$ (V/s) is the scan rate in CV experiments.
[21] A. J. Bard, L. R. Faulkner, *Electrochemical Methods. Fundamentals and Applications*, Wiley, New York, **1980**, chapter 11, pp. 429−485; E. R. Brown, R. F. Large, in: *Techniques of Chemistry*, Volume I − *Physical Methods of Chemistry*, Part IIA (Ed.: A. Weissberger), Wiley, **1971**, chapter 6, pp. 423−530.
[22] W. H. Baur, K. Wieghardt, *J. Chem. Soc., Dalton Trans.* **1973**, 2669−2674.
[23] J. D. Edwards, K. Wieghardt, A. G. Sykes, *J. Chem. Soc., Dalton Trans.* **1974**, 2198−2204.
[24] C. Grünwald, M. Laubender, J. Wolf, H. Werner, *J. Chem. Soc., Dalton Trans.* **1998**, 833−839.
[25] B. K. Das, A. R. Chakravarty, *Inorg. Chem.* **1991**, *30*, 4978−4986.
[26] T. Arliguie, B. Chaudret, G. Chung, F. Dahan, *Organometallics* **1991**, *10*, 2973−2977.
[27] D. Lee, P.-L. Hung, B. Spingler, S. J. Lippard, *Inorg. Chem.* **2002**, *41*, 521−531.
[28] The design of the electrochemical cell used throughout did not allow the detection of $H_2$ (a possible product of the oxidation of **2** by protons) because a dinitrogen or argon stream was continuously circulating over the solution during the experiments.
[29] This statement is made on the reasonable assumption that the diffusion coefficients of the μ-OH and μ-Cl complexes are similar.
[30] Y. Alias, S. K. Ibrahim, M. A. Queiros, A. Fonseca, J. Talarmin, F. Volant, C. J. Pickett, *J. Chem. Soc., Dalton Trans.* **1997**, 4807−4815.
[31] D. L. Hughes, M. Y. Mohammed, C. J. Pickett, *J. Chem. Soc., Chem. Commun.* **1988**, 1481−1482.

  

[32] The fact that *n* is slightly larger than the theoretical value (2.0) when the electrolysis potential is −0.9 V can be attributed to the fact that small amounts of $\mathbf{2}^{+}$ produced by protonation of **2** (see Schemes 5 and 8) are reduced back to **2**. The extra charge consumed thus results in the reduction of $H^{+}$ to H[28] via the $\mathbf{2}^{+}/\mathbf{2}$ couple. When the electrolysis is performed at a potential which does not allow the $\mathbf{2}^{+} \rightarrow \mathbf{2}$ reduction ($E_{el} = -0.5$V), the charge consumed is $n \leq 2$ F·mol$^{-1}$ $\mathbf{1}^{+}$.
[33] M. E. Noble, J. C. Huffman, R. A. D. Wentworth, *Inorg. Chem.* **1983**, *22*, 1756−1760; M. E. Noble, K. Folting, J. C. Huffman, R. A. D. Wentworth, *Inorg. Chem.* **1984**, *23*, 631−634.
[34] A. Neves, U. Bossek, K. Wieghardt, B. Nuber, J. Weiss, *Angew. Chem. Int. Ed. Engl.* **1988**, *27*, 685−687.
[35] J. H. Shin, G. Parkin, *Chem. Commun.* **1998**, 1273−1274.
[36] F. Demirhan, P. Richard, R. Poli, *Inorg. Chim. Acta* **2003**, *347*, 61−66.
[37] F. Bottomley, J. Chen, *Organometallics* **1992**, *11*, 3404−3411.
[38] G.-H. Pan, B.-T. Zhuang, Q. Wei, Z.-F. Zhou, S.-Q. Peng, K.-C. Wu, J.-T. Chen, *Chinese J. Struct. Chem.* **2001**, *20*, 381−383; G. Pan, B. Zhuang, J. Chen, *Acta Crystallogr. Sect. C* **1999**, *55*, 298−300; G. Pan, B. Zhuang, J. Chen, *Acta Crystallogr. Sect. C* **1998**, *54*, 1580−1582.
[39] Programs used: *SHELX97* − Programs for Crystal Structure Analysis (Release 97−2). G. M. Sheldrick, Institut für Anorganische Chemie der Universität Göttingen, Tammanstrasse 4, 3400 Göttingen, Germany, **1998**, *WinGX* − A Windows Program for Crystal Structure Analysis: L. J. Farrugia, *J. Appl. Crystallogr.* **1999**, *32*, 837.
[40] Programs used for CV simulations: ESP (Electrochemical Simulations Package v. 2.4) from Carlo Nervi (http://lem. ch. unito. it/chemistry/esp manual. html) or Virtual CV 1.0 (available on the worldwide web as vTLCv10.zip) from André Laouénan.

Received October 7, 2003
Early View Article
Published Online March 5, 2004

  